Kinematics of Circumgalactic Gas

Martin et al. arxiv:1901.09123

	Galaxy Evolution Topic	2020s Advances	Circumgalactic Relevance	Needed CGM Information
1	Morphologies and Internal Kinematics	Spatially resolved maps in ISM and stars to fainter sources, higher redshifts, smaller spatial scales	Angular momentum exchange; dynamical and thermal state of gas accreting onto ISM	Spatially resolved CGM kinematics with respect to galaxies' resolved kinematics
2	Star Formation Histories	Spatially resolved SFHs to smaller scales and higher redshifts; improved SED modeling	Fuel (or lack thereof) for star formation comes from the CGM	Accretion rates, morphologies, kinematics, and thermodynamics
3	Chemical Evolution	Spatially resolved ISM metallicity maps for more galaxies, earlier epochs; more resolved stellar populations in Milky Way and the local universe	Most heavy elements are in CGM. Accretion dilutes ISM; recycling & outflows redistribute metals.	Understand metallicity substructure & mixing; distribution & dynamics of metals
4	Quenching	Improved understanding of quenching *within* galaxies, environmental dependence, co-evolution with SMBHs	CGM drives or impacted by quenching event; source of any gas accreting onto galaxies	Thermodynamics of gas in the CGM of quenching and quenched galaxies
5	Satellite Evolution	Lower masses outside of Local Group; earlier epochs; more detailed SFHs	Satellites are traveling through central galaxies' CGM	Spatially and spectrally resolved maps to determine density and kinematic structure
6	The Dark Matter Halo Connection	Deep large-scale structure surveys in visible and near-infrared	CGM modulates how/if gas accreted onto halo reaches the ISM	CGM gas distribution for different kinds of galaxies at all epochs
7	Reionization	Map it; determine sources, morphology, redshift range, rate	Affects how much ionizing flux escaping galaxies reach the IGM	Small-scale structure and opacities to ionizing flux

sample selection

- 0.15<z<0.3
- u-r < 2.0
- b/a < 0.71
- u(QSO) < 18.5
- rp < 100kpc
  (prioritized rp < 60 kpc)

observed:

50 galaxy – quasar pairs

KECK : NIRC2 & LRIS (50)

HST : F390W & F814W(9)

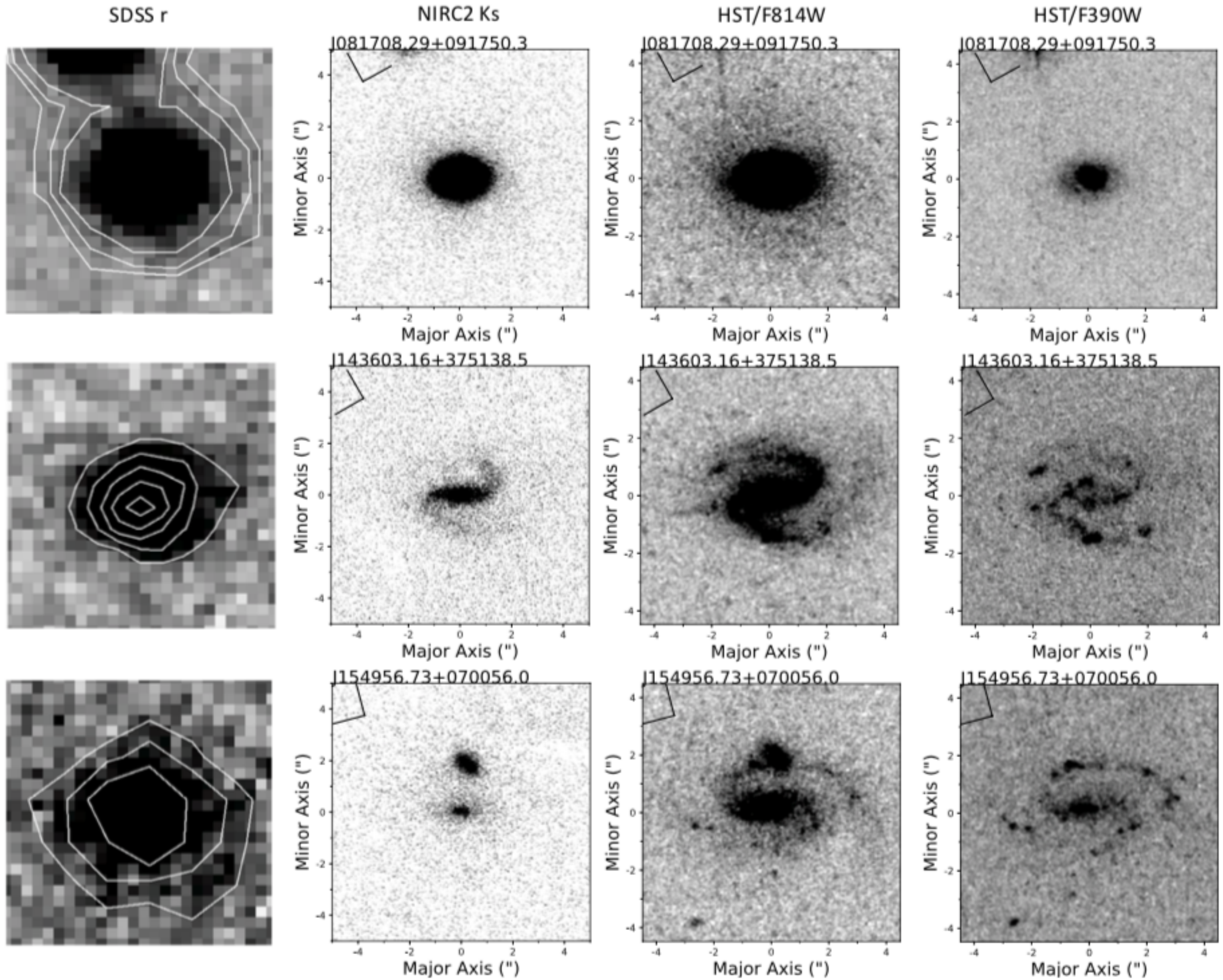

SDSS r
NIRC2 Ks
HST/F814W
HST/F390W
J081708.29+091750.3
J143603.16+375138.5
J154956.73+070056.0
Minor Axis (")
Major Axis (")

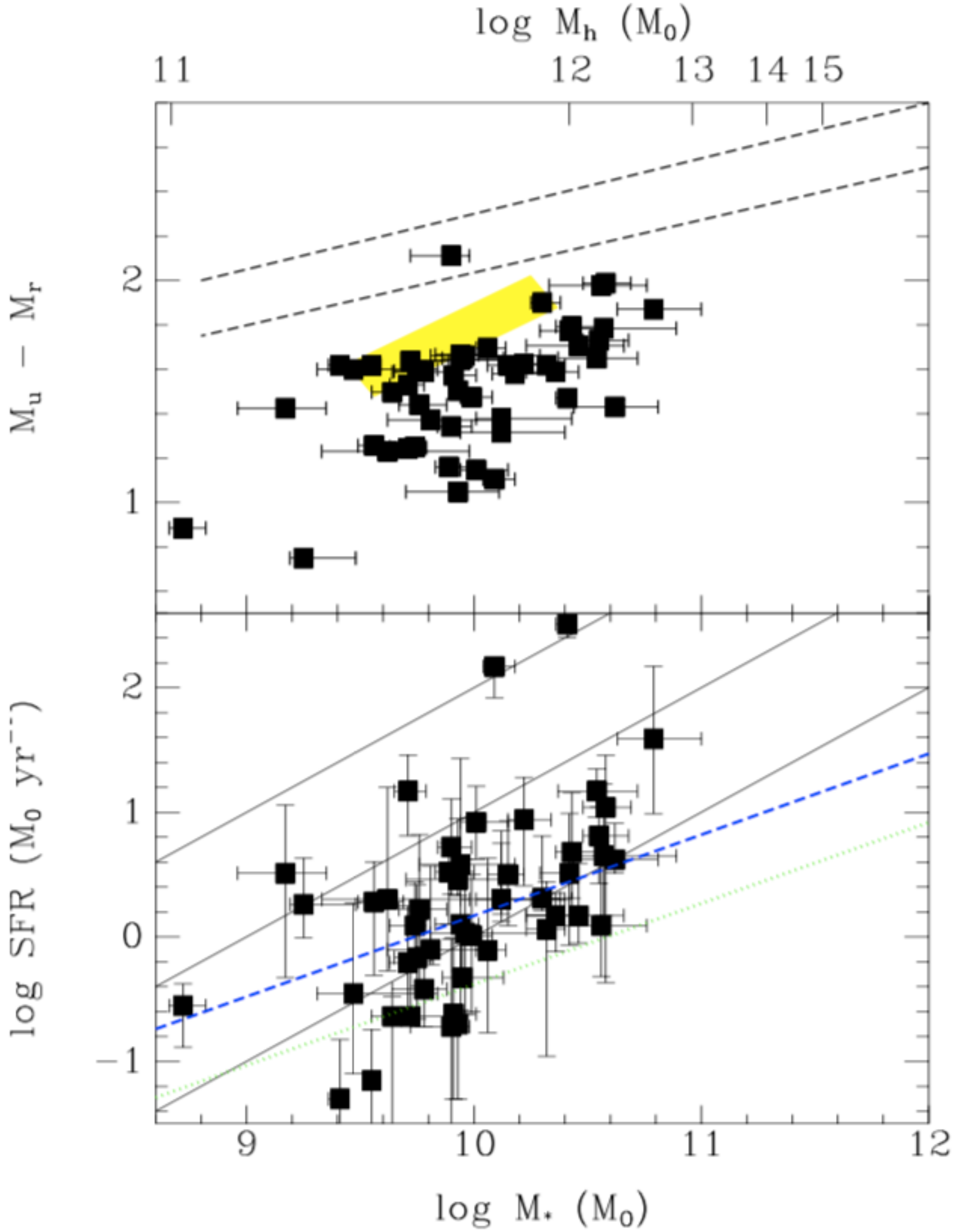

log M_h (M_0)
11
12
13
14
15
M_u − M_r
2
1
log SFR (M_0 yr⁻¹)
2
1
0
−1
9
10
11
12
log M_* (M_0)

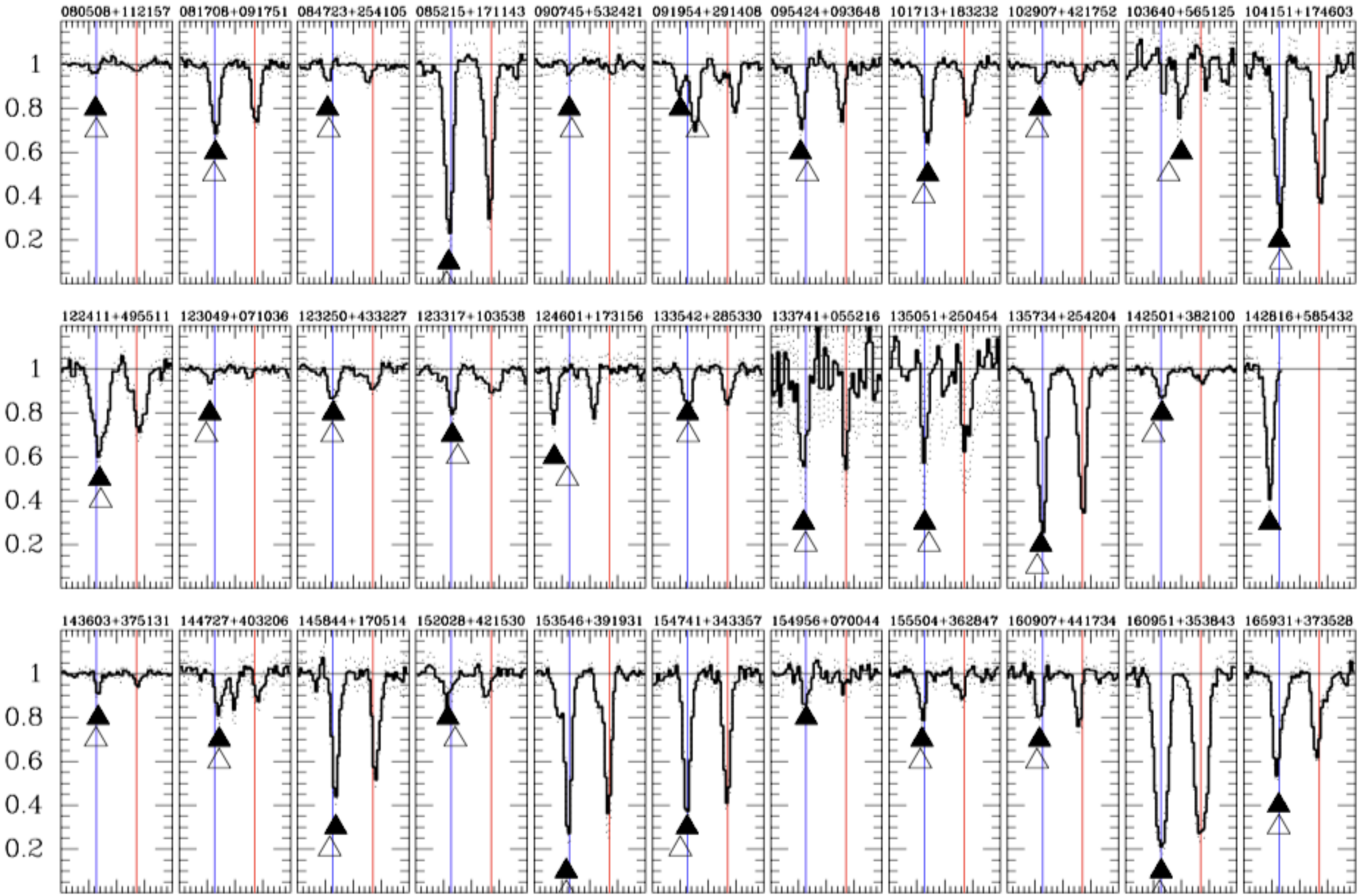

Figure 5. Continuum normalized quasar spectra showing Mg II system near the target galaxy redshift. Each spectrum has

Mg II 2796 2803 absorption lines

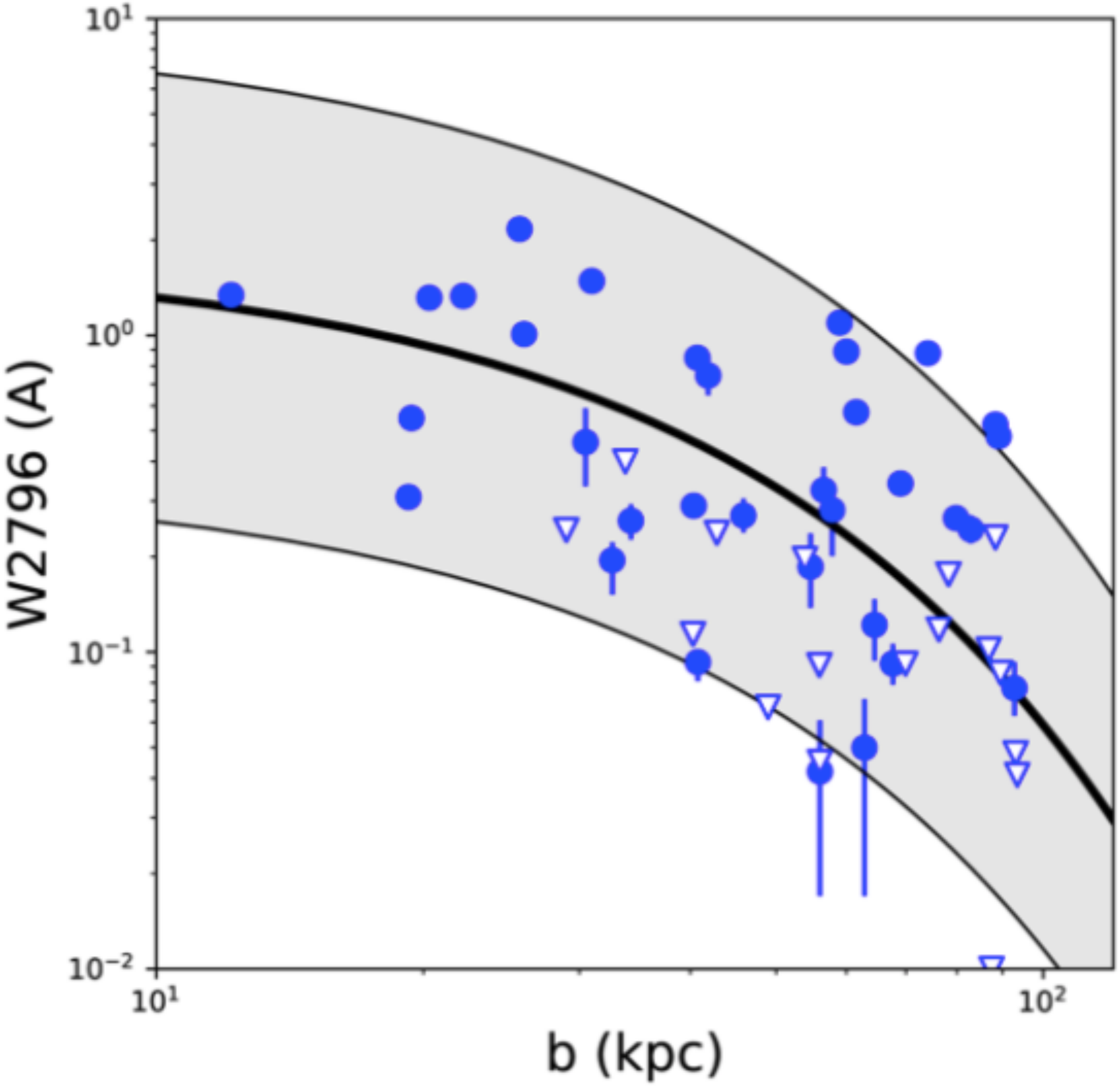

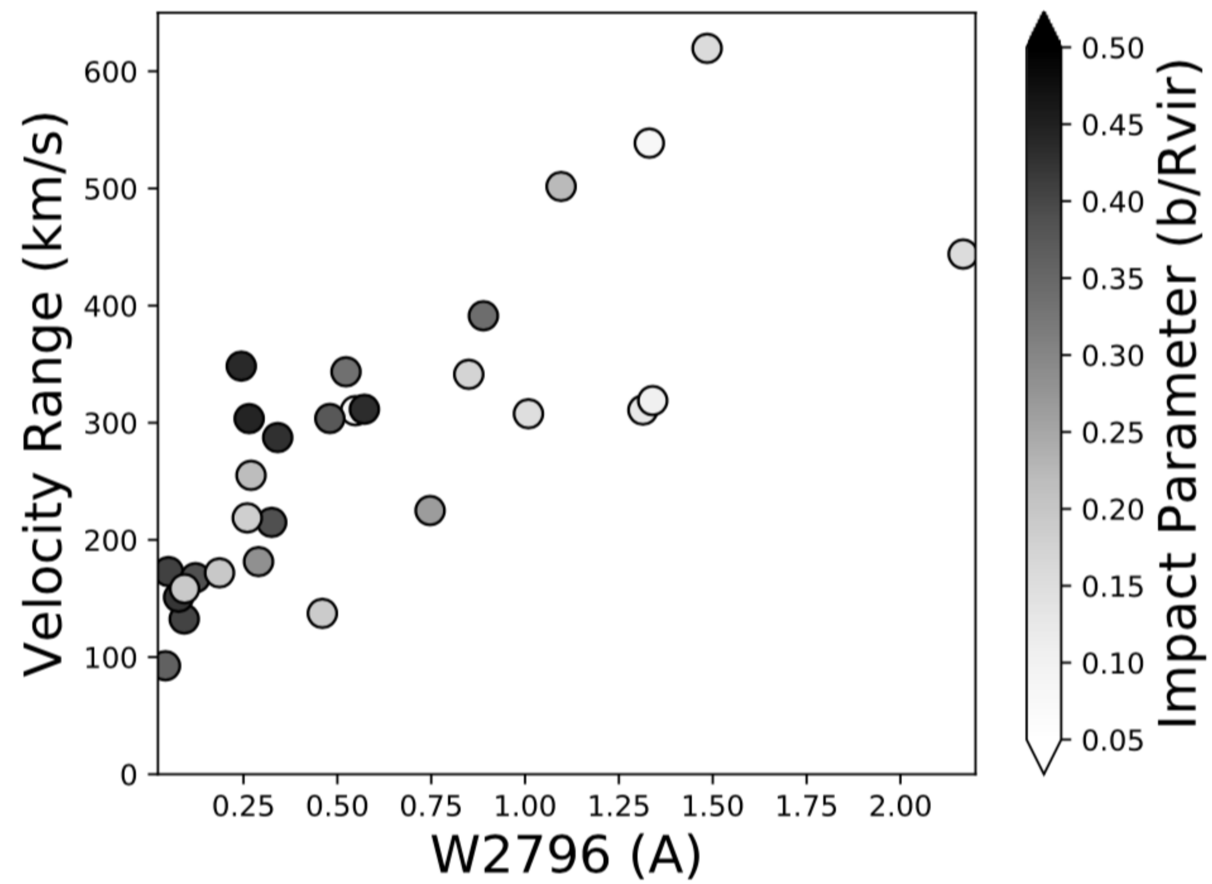

Figure 6. Rest-frame equivalent width of Mg II 2796 versus impact parameter. Absorption strength declines with the distance of the sightline from the galaxy, consistent with previous studies. For comparison, the black line shows the maximum likelihood fit from Nielsen et al. (2013); the shaded region shows the root-mean-square variation between this fit and their sample.

$$\Delta W(\lambda 2796) \equiv W_r / \langle W(b) \rangle$$

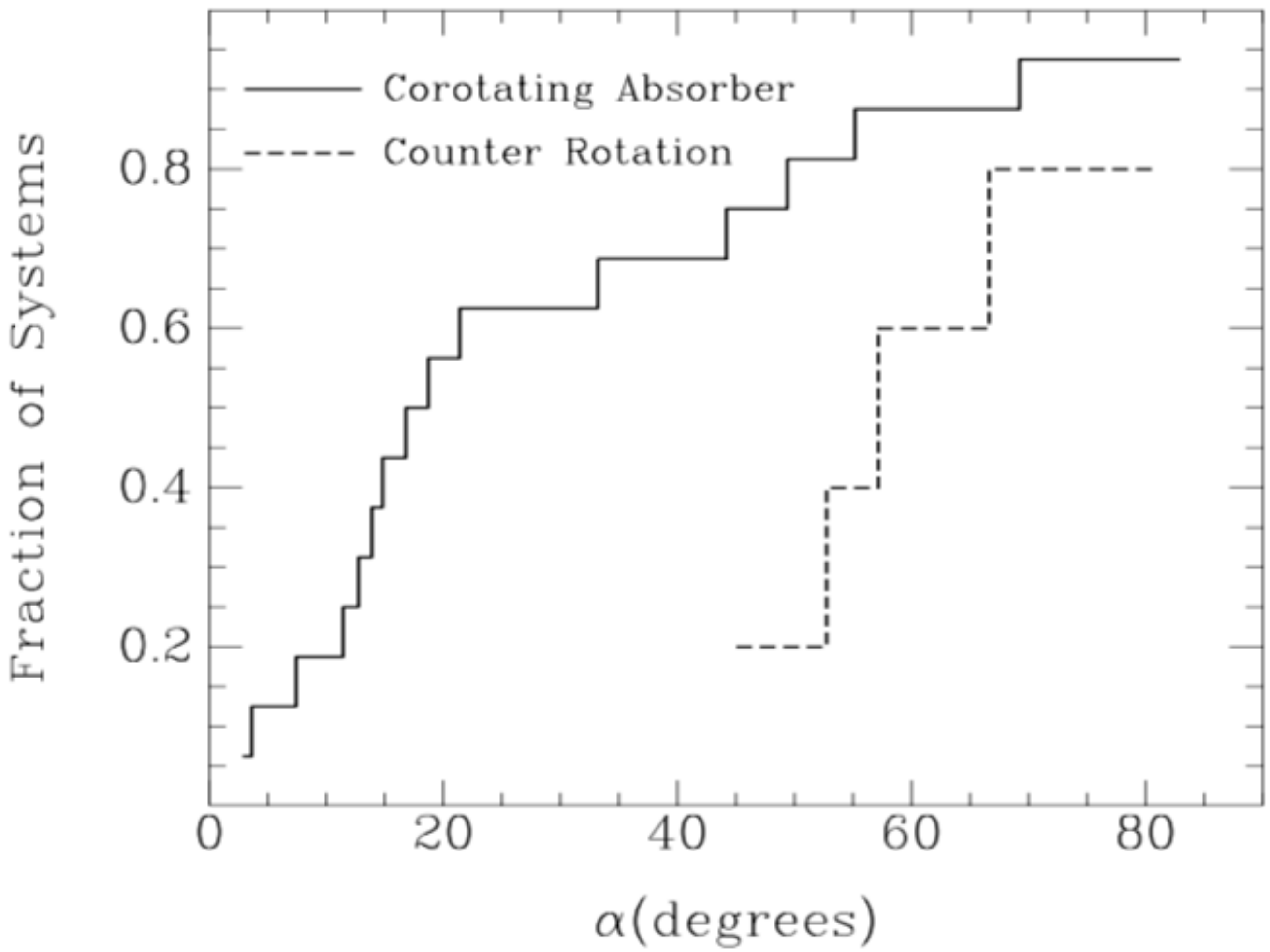

No counter-rotation of the CGM is detected within 45° of the major axis at any impact parameter

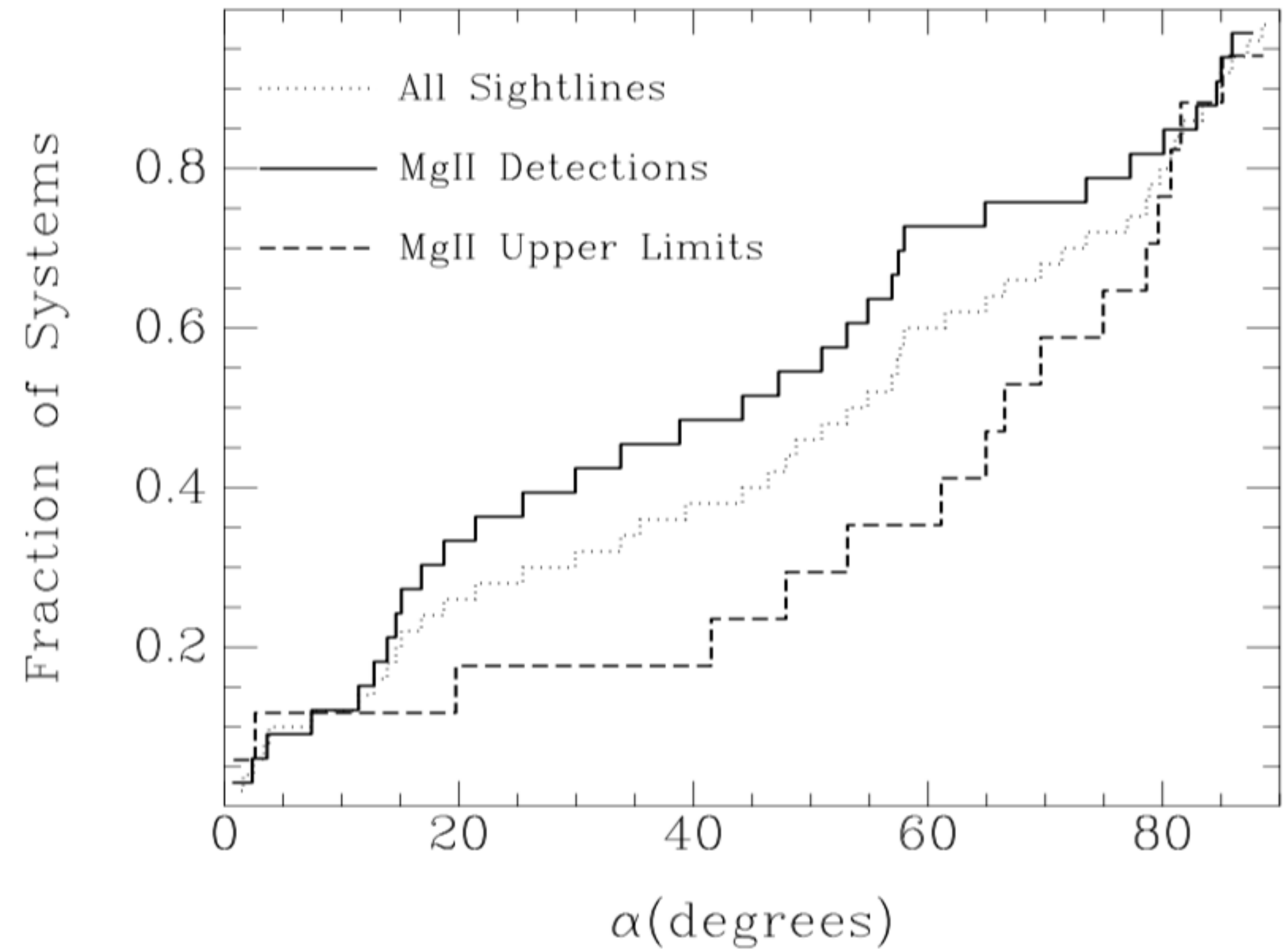

The paucity of non-detections at low α means high covering factor of strong Mg II absorption

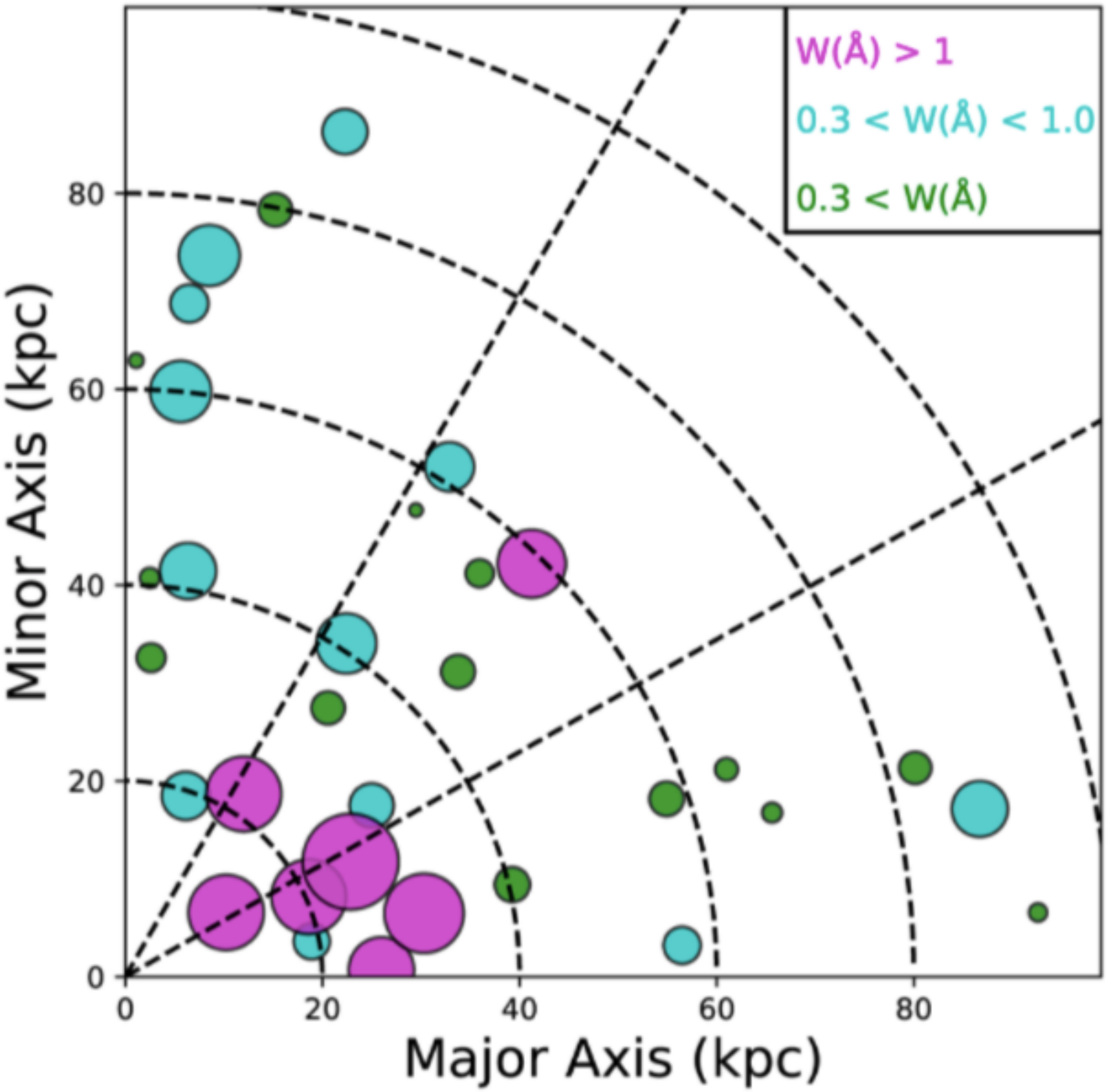

The very strong may intersect extended disks

The strong absorbers confirm that absorption strength increases near the minor axis.

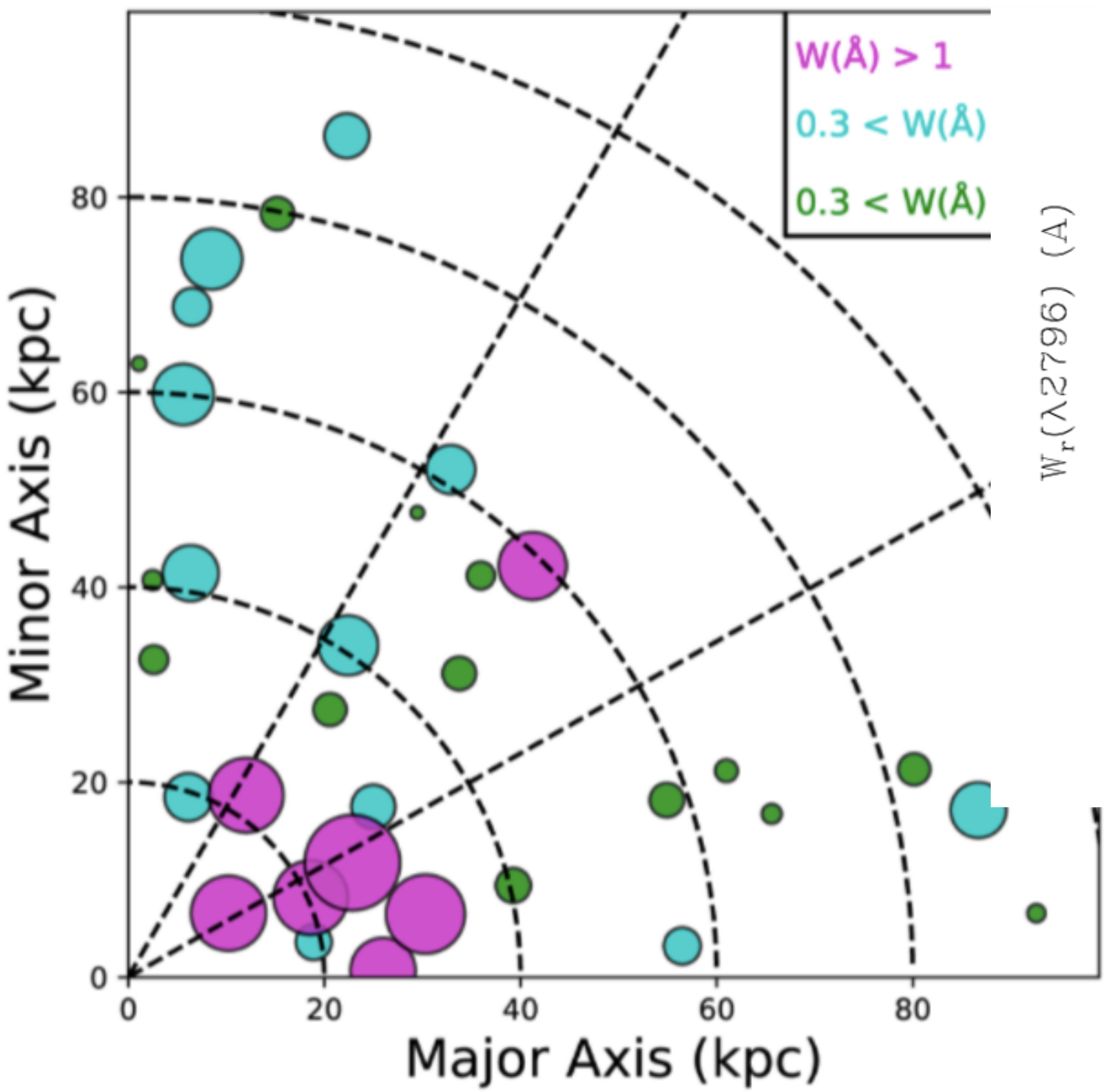

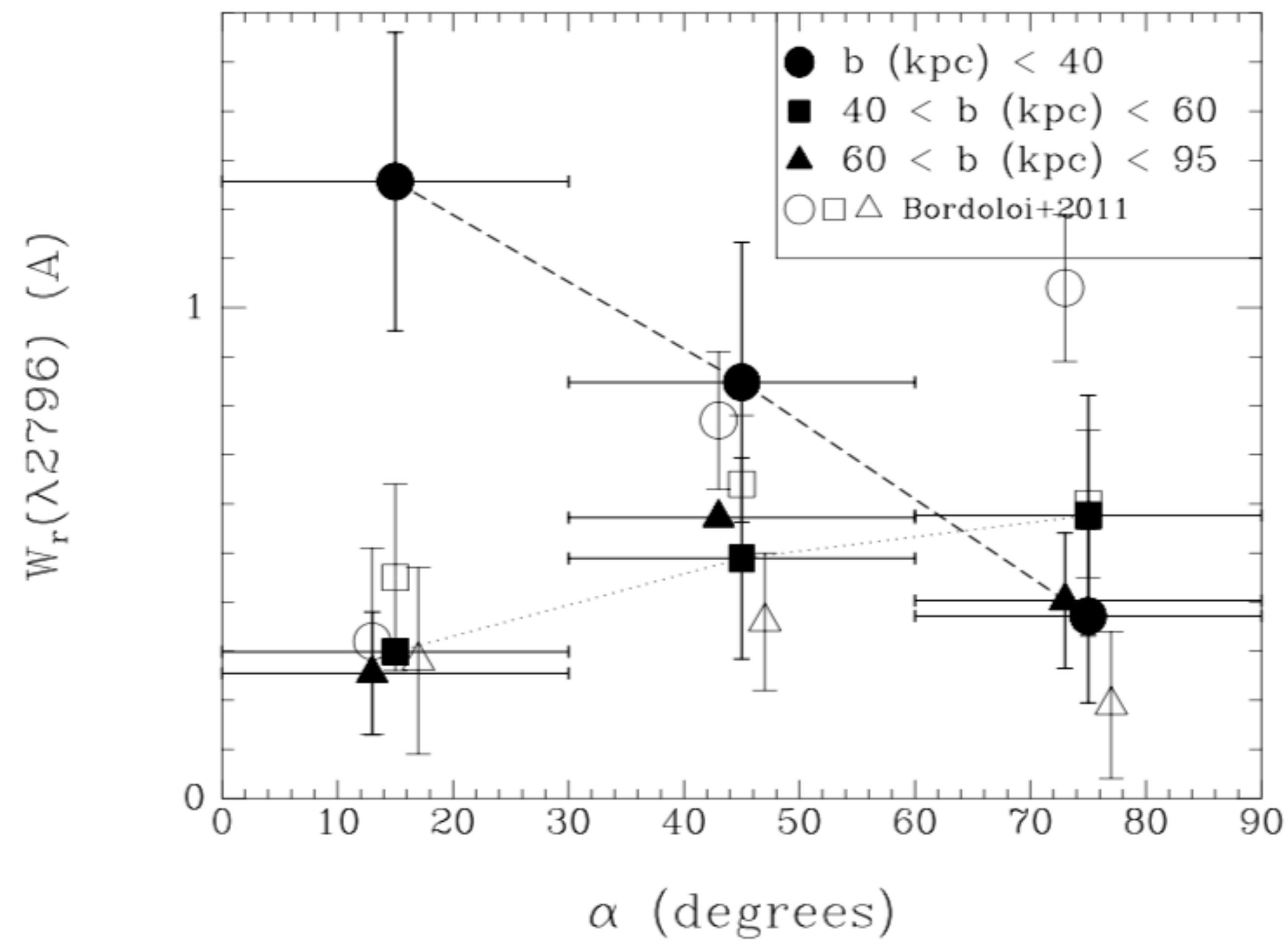

The very strong may intersect extended disks

The strong absorbers confirm that absorption strength increases near the minor axis.

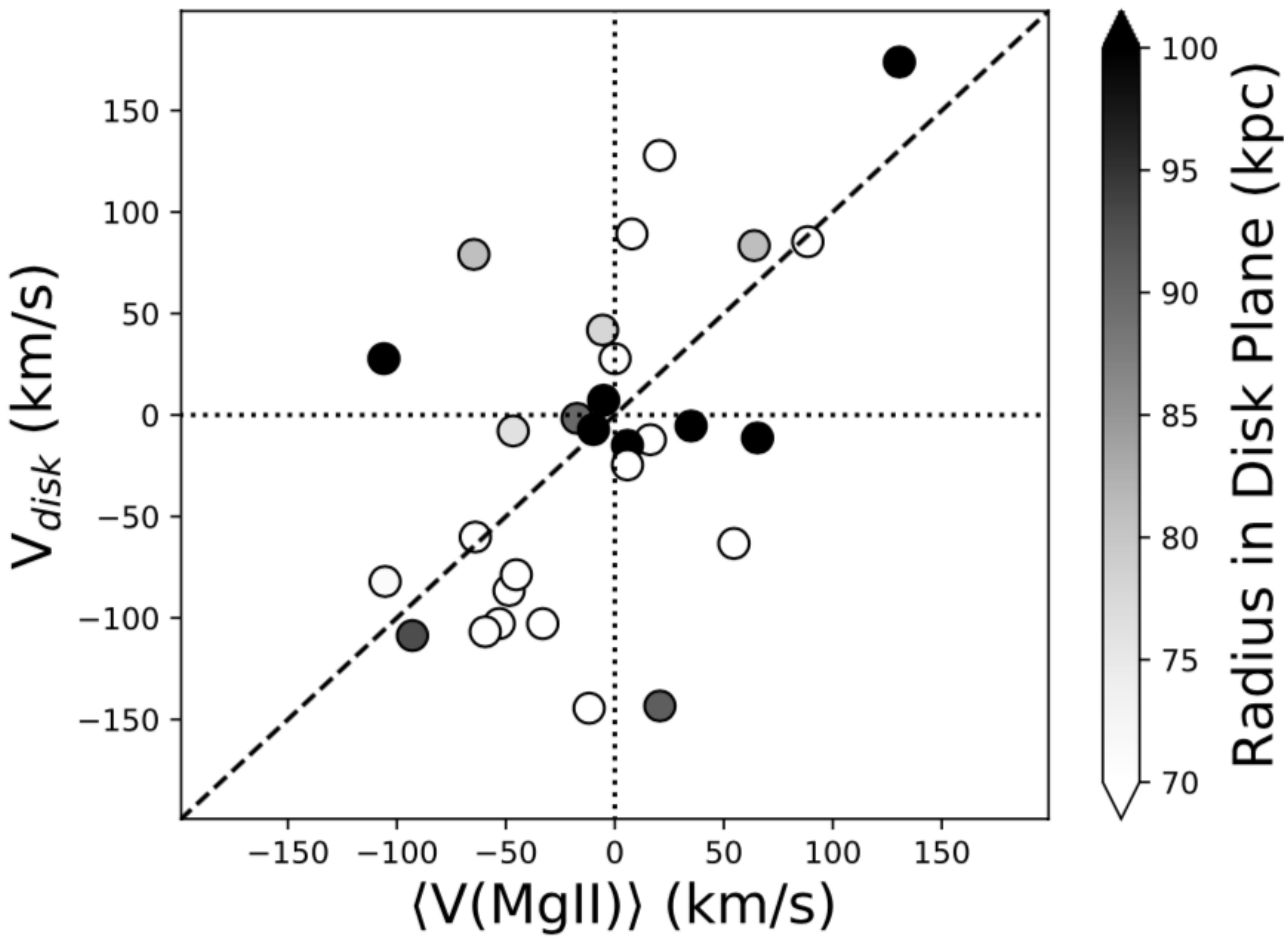

$R_{max} \approx \; 80 \pm 10$ kpc.

The positive correlation is strongest at radii R < Rmax

Centrifugal force support of the low-ionization CGM is significant out to at least Rmax

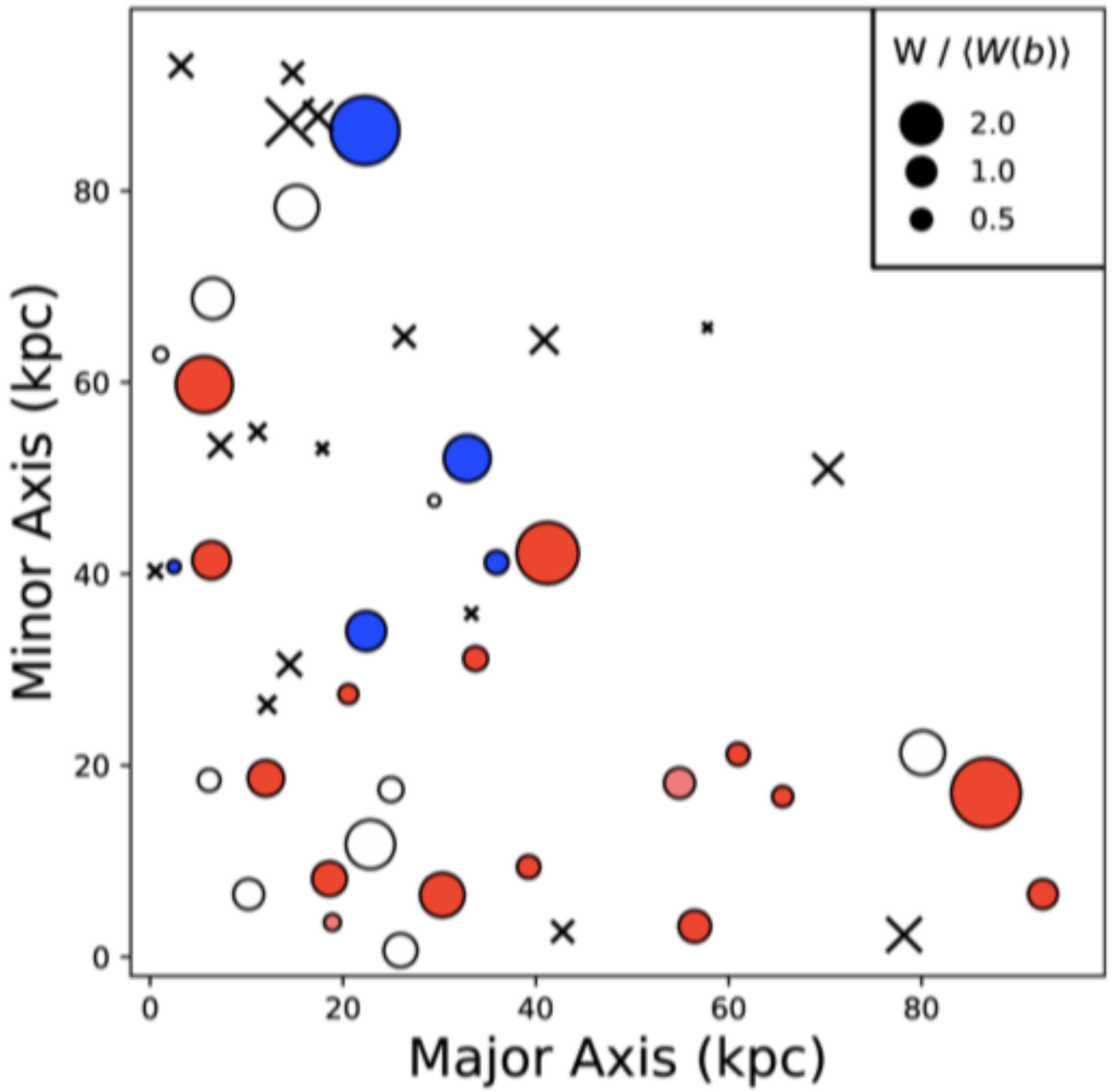

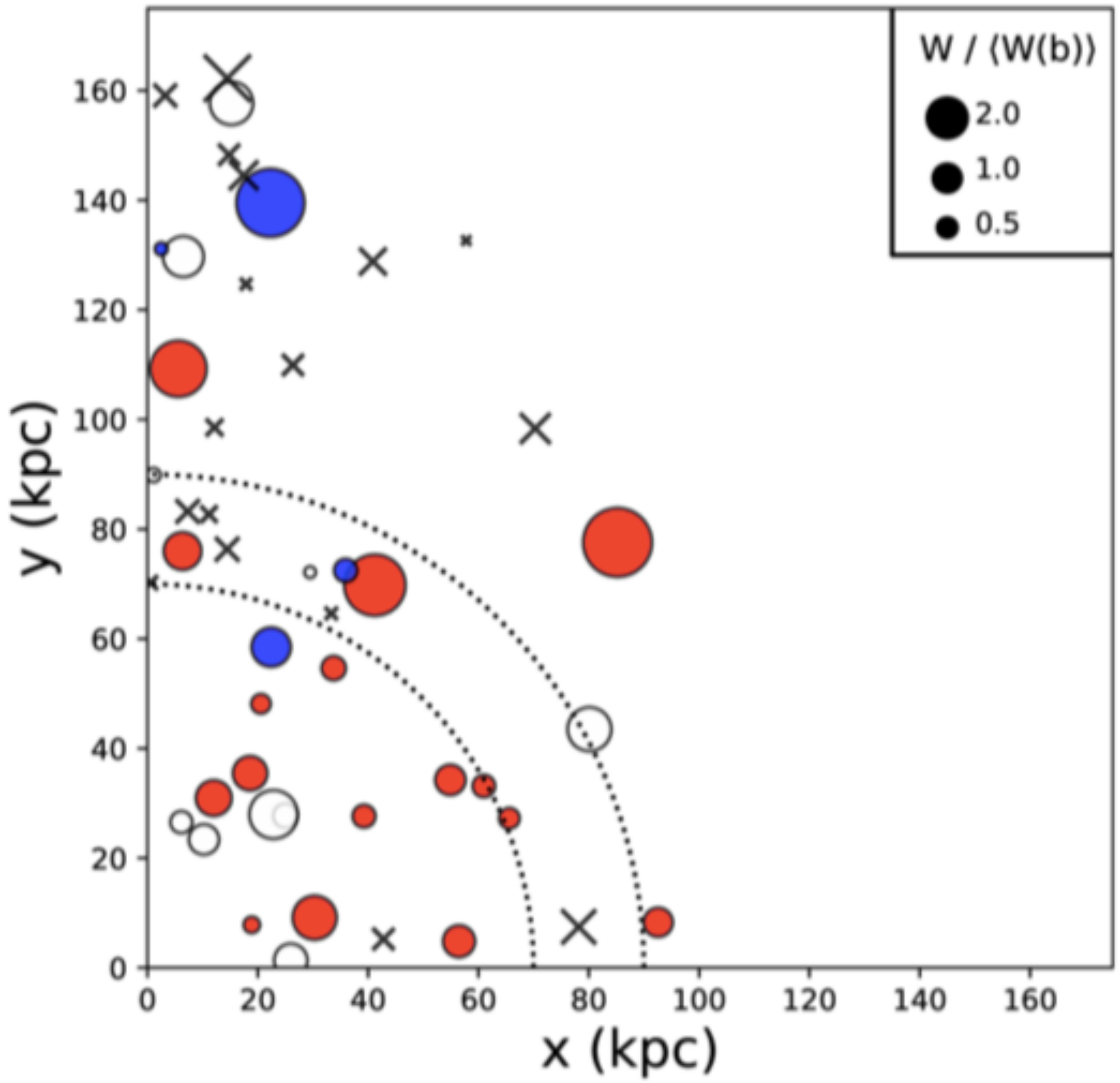

large EW excess is found most often along α > 45° and b > 40 kpc.

absorption from extended disk is unlikely to be the primary source of the excess

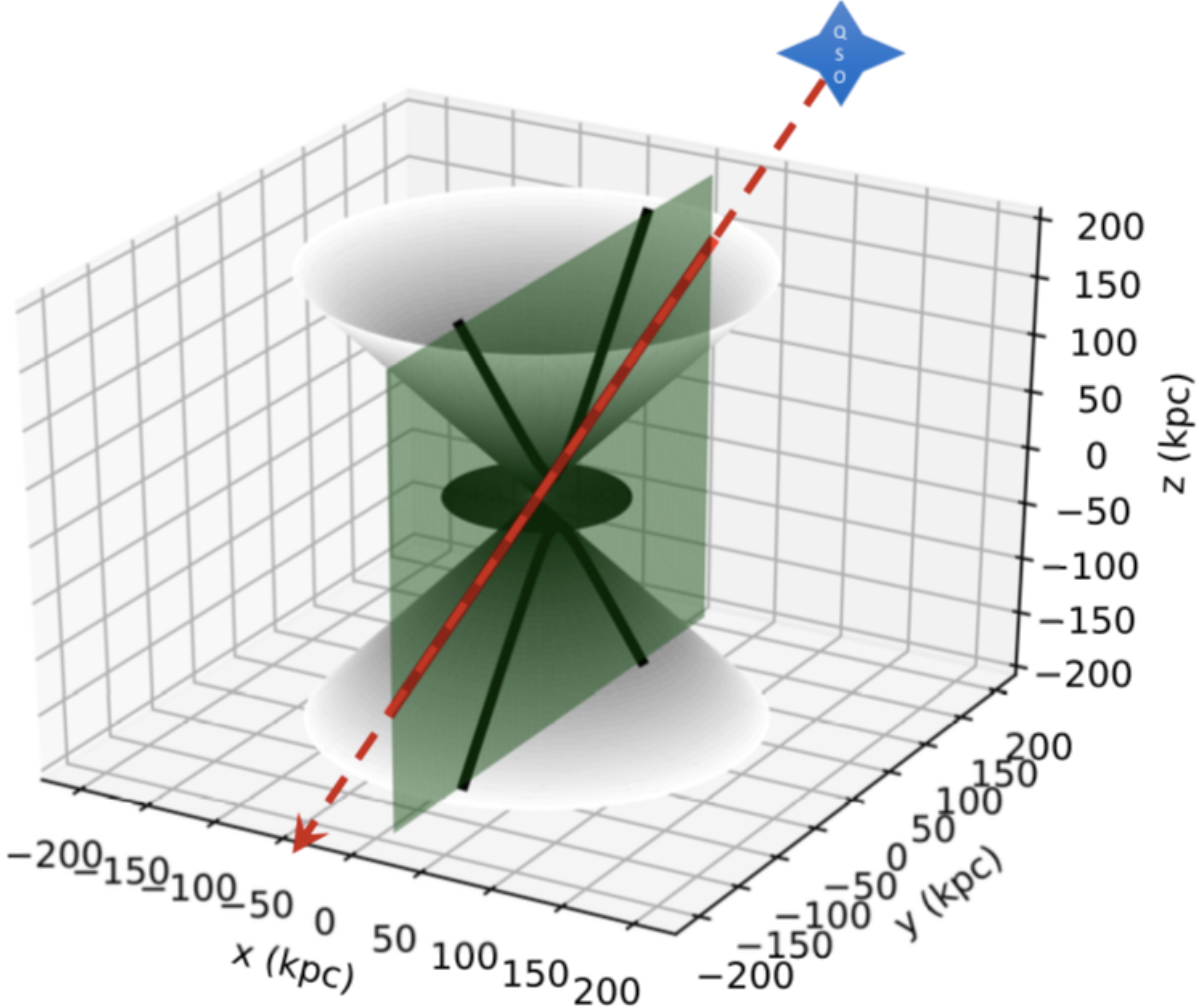

3D geometry of a galactic disk and bipolar outflow

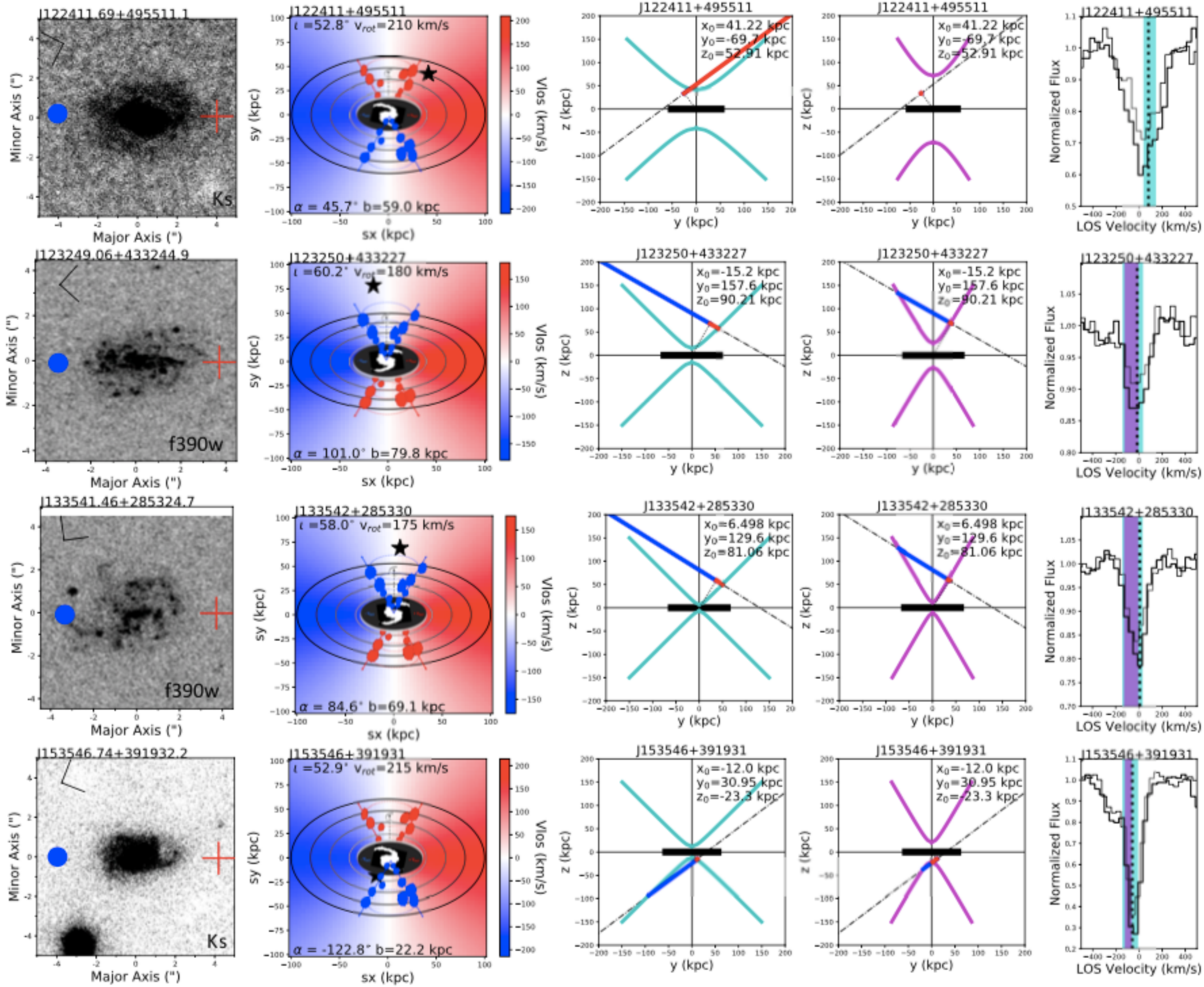

J122411.69+495511.1
Ks
J122411+495511
ι =52.8° v_rot=210 km/s
α = 45.7° b=59.0 kpc
x0=41.22 kpc
y0=-69.7 kpc
z0=52.91 kpc
J123249.06+433244.9
f390w
J123250+433227
ι =60.2° v_rot=180 km/s
α = 101.0° b=79.8 kpc
x0=-15.2 kpc
y0=157.6 kpc
z0=90.21 kpc
J133541.46+285324.7
f390w
J133542+285330
ι =58.0° v_rot=175 km/s
α = 84.6° b=69.1 kpc
x0=6.498 kpc
y0=129.6 kpc
z0=81.06 kpc
J153546.74+391932.2
Ks
J153546+391931
ι =52.9° v_rot=215 km/s
α = -122.8° b=22.2 kpc
x0=-12.0 kpc
y0=30.95 kpc
z0=-23.3 kpc
Minor Axis (")
Major Axis (")
sy (kpc)
sx (kpc)
Vlos (km/s)
z (kpc)
y (kpc)
Normalized Flux
LOS Velocity (km/s)

summary

- The Mg II absorbers often show a net Doppler shift with the same sign as the galactic rotation;
  Differences between corotators and counter-rotators depend on galaxy inclination
- Absorber strengths at fixed impact parameter generally increase with azimuthal angle
- Angular mo- mentum in supporting the low-ionization CGM
- Galactic outflows produce most of the equivalent width